Published in final edited form as:
Glia. 2010 April 15; 58(6): 633–649. doi:10.1002/glia.20950.

A novel type of glial cell in the retina is stimulated by insulin-like growth factor 1 and may exacerbate damage to neurons and Müller glia

Andy J. Fischer, **Melissa A. Scott**, **Christopher Zelinka**, and **Patrick Sherwood**
Department of Neuroscience, The Ohio State University, Columbus, OH

Abstract

Recent studies have demonstrated that insulin can have profound affects upon the survival of neurons within the retina. The purpose of this study was to determine how insulin-like growth factor 1 (IGF1) influences retinal cells; in particular the glial cells. We identify a novel type of glial cell in the avian retina and provide evidence these cells respond to acute damage and IGF1. In normal retinas, we found a distinct cell-type, scattered across the ganglion cell and inner plexiform layers, that expressed Sox2, Sox9, Nkx2.2, vimentin and transitin, the avian homologue of mammalian nestin. These glial cells have a unique immunohistochemical profile, morphology and distribution that are distinct among other known types of retinal glia, including microglia, oligodendrocytes, astrocytes and Muller glia. We termed these cells Non-astrocytic Inner Retinal Glia-like (NIRG) cells. We found that the NIRG cells may express the IGF1 receptor and respond to IGF1 by proliferating, migrating distally into the retina, and up-regulating transitin. In addition, IGF1 stimulated microglia to become reactive and up-regulate lysosomal membrane glycoprotein and CD45. With microglia and NIRG cells stimulated by IGF1 there were elevated levels of cell death and numerous focal detachments across the retina in response to excitotoxic damage. Cell death was prominent within areas of detachment coinciding with a stark loss of Müller glia and accumulation of NIRG cells. We conclude that NIRG cells are a novel type of retinal glia that is sensitive to IGF1 and whose activity may impact the survival of neurons and Müller glia.

Keywords

retina; Müller glia; microglia; IGF1; Nkx2.2; Sox2; Sox9

Introduction

Müller glia are the predominant type of support cell in the retina, providing structural, nutritive and metabolic support to neurons. Accordingly, the activity of the Müller glia impacts the function and survival of retinal neurons. The aberrant activity of Müller glia often occurs with retinal disease (Bringmann et al. 2006; Bringmann and Reichenbach 2001; Giaume et al. 2007). The activity of Müller glia dramatically changes in damaged retinas or when stimulated by exogenous growth factors (reviewed by Bringmann et al. 2006; Fischer 2005; Giaume et al. 2007). The identities of secreted factors that influence the activity of Müller glia in the retina are slowly being revealed. For example, we have demonstrated that the combination of insulin and FGF2, but neither factor alone, causes Müller glia to de-differentiate, proliferate, express transcription factors normally expressed by retinal

Corresponding author: Andy J. Fischer, Department of Neuroscience, Ohio State University, College of Medicine, 4190 Graves Hall, 333 W. 10th Ave, Columbus, OH 43210-1239, USA. Telephone: (614) 292-3524; Fax: (614) 688-8742; fischer.412@osu.edu.

progenitors, and produce a few new neurons (Fischer et al. 2002). FGF2 alone selectively stimulates Müller glia to accumulate pERK1/2, p38 MAPK, pCREB, cFos and Egr1 (Fischer et al. 2009a). Following stimulation of Müller glia with FGF2, retinal neurons are protected against an excitotoxic insult (Fischer et al. 2009a). By comparison, intraocular injections of insulin stimulate microglia-like cells to up-regulate transitin and lysosomal membrane glycoprotein (LMG), and Müller glia to up-regulate cFos and Egr1 (Fischer et al. 2009a). Insulin-treatment renders retinal neurons more susceptible to damage in response to an excitotoxic insult (Fischer et al. 2009a). However, insulin receptors are not expressed by cells in the chicken retina (Fischer et al. 2009a). Thus, it is assumed that insulin influences retinal cells by acting at receptors for insulin-like growth factors (IGFs). However, the effects of IGFs upon retinal cells remain uncertain.

In addition to Müller cells, glial cell-types within the retina include microglia, astrocytes and oligodendrocytes. The retinas of all classes of vertebrates contain resident populations of microglia which are normally found scattered throughout the inner and outer plexiform layers (reviewed by Giaume et al. 2007). In vascular retinas numerous astrocytes are closely associated with blood vessels (reviewed by Friedlander et al. 2007). Astrocytes and oligodendrocytes are known to migrate into the retina from the optic nerve; these glia are not generated by retinal progenitors (Barres and Raff 1993; Barres and Raff 1999). The types of glial cells differ in avascular retinas, such as those of chickens, guinea pigs and rabbits. In avascular retinas there are few, if any, astrocytes present (Prada et al. 1998; Won et al. 2000). Interestingly, some of the axons in the Nerve Fiber Layer (NFL) are myelinated by oligodendrocytes in avascular retinas (Tsai and Miller 2002; Won et al. 2000).

Here we identify a novel type of glial cell in the avian retina. This cell has a unique morphology, distribution within the retina, and phenotype. We termed these cells Non-astrocytic Inner Retinal Glia-like (NIRG) cells. We find that IGF1 stimulates the NIRG cells, as well as microglia, and this treatment increases the vulnerability of retinal neurons and Müller glia to an excitotoxic insult.

Materials and Methods

Animals

The use of animals in these experiments was in accordance with the guidelines established by the National Institutes of Health and the Ohio State University. Newly hatched leghorn chickens (*Gallus gallus domesticus*) were obtained from the Department of Animal Sciences at The Ohio State University. The chicks were kept on a cycle of 12 hours light, 12 hours dark (lights on at 7:00 am). Chicks were housed in a stainless steel brooder at about 28°C and received water and Purina^{tm} chick starter *ad libitum.*

Intraocular injections

Intravitreal injections were performed as described previously (Fischer et al. 1999; Fischer et al. 1998). In all experiments, 20 μl of vehicle containing the test compound was injected into the experimental (left) eye, and 20 μl of vehicle alone was injected into the control (right) eye. The vehicle was sterile saline containing bovine serum albumin, 50 μg/ml, as carrier, and 5-bromo-2′-deoxyurdiine (BrdU; 100 μg/ml) to label proliferating cells. Test compounds included N-methyl-D-aspartate (NMDA; 1 or 2 μg per dose; Sigma-Aldrich), recombinant human IGF1 (300–800 ng/dose; R&D Systems) and recombinant human IGF2 (300–800 ng/dose; R&D Systems).

We used 3 different injection paradigms: (1) on P5 and P6 the left eye received an injection of factor and the right eye received vehicle. Retinas were harvested 24 hrs after the last injections. (2) on P5 and P6 the left eye received an injection of factor and the right eye

received vehicle. On P7, both eyes received an injection of 1 μmol NMDA. On P8, both eyes received an injection of 2 μg BrdU, and retinas were harvested 4 hrs later. (3) on P5 and P6 the left eye received an injection of factor and the right eye received vehicle. On P7, both eyes received an injection of 1 μmol NMDA. On P9, both eyes received an injection of 2 μg BrdU, and retinas were harvested 24 hrs later on P10.

Reverse transcriptase PCR

Retinas from 2 P7 chicks were pooled and placed in 1.5 ml of Trizol Reagent (Invitrogen) and total RNA was isolated according to the Trizol protocol and resuspended in 50 μl RNAse free water. Genomic DNA was removed by using the *DNA FREE* kit provided by Ambion. cDNA was synthesized from mRNA by using Superscript^{tm} III First Strand Synthesis System (Invitrogen) and oligo dT primers according to the manufacturer's protocol. Control reactions were performed using all components with the exception of the reverse transcriptase to exclude the possibility that primers were amplifying genomic DNA.

PCR primers were designed by using the web-based program Primer 3 from the Whitehead Institute for Biomedical Research (http://frodo.wi.mit.edu/). Primer sequences are as follows: IGF1R – forward 5′ GGC AAA GCT GAC ACA TCT GA 3′ – reverse 5′ TCC AGG TCA AGC TCC TCT GT 3′; IGF2R forward 5′ GCT GGA TGT GAA GCA GAC AA 3′ – reverse 5′ GCC TCC CAG TTC TCT CTG TG 3′. Predicted product sizes (in base pairs) were 1221 (IGFR1) and 1199 (IGFR2). PCR reactions were performed by using standard protocols, Platinum^{tm} Taq (Invitrogen) and an Eppendorf thermal cycler. PCR products were run on an agarose gel to verify the predicted product sizes, TOPO-cloned (as described below) and sequenced to verify the identity of the products.

TOPO cloning

PCR products were produced with Platinum^{tm} Taq polymerase (Invitrogen), run on a 1.2% agarose gel, extracted and purified by using Qiagen's Qiaex II kit according to the manufacturer's instructions. TOPO cloning was performed using Invitrogen's TOPO TA^{tm} Cloning Kit and the pCR–II vector according to manufacturer's instructions.

In situ hybridization

Standard procedures were used to generate DIG-labeled riboprobes and for *in situ* hybridization, as described previously (Fischer et al. 2008a; Fischer et al. 2008b).

RCA1 labeling

Vertical sections of the retina were ringed with rubber cement and washed 15 minutes in PBS + 0.1% Tween20. Following 2 additional washes in PBS, sections were incubated under Biotinylated Ricinus Communis Agglutinin I (RCA1; Vector Laboratories) diluted to 1.7 μg/ml in PBS for 1 hr at 38°C in a humidified chamber. Slides were washed once in PBS at 38°C, washed once in PBS at room temperature, and incubated for 30 minutes under Streptavidin-Alexa488 (Invitrogen) diluted to 1:2000. Finally, slides were washed 2 times in PBS and then either mounted with coverglass or processed for indirect immunofluorescence.

Fixation, sectioning and immunocytochemistry

Tissue were fixed, sectioned and immunolabeled as described previously (Fischer et al. 2008a). Whole-mount preparations of retinas were fixed and processed as described previously (Fischer et al. 2006). Working dilutions and sources of antibodies used in this study are listed in Table 1. We evaluated the specificity of primary antibodies by comparison with published examples of results and assays for specificity. None of the observed labeling appeared to be due to secondary antibody or fluorophore because sections

labeled with secondary antibodies alone were devoid of fluorescence. Secondary antibodies included donkey-anti-goat-Alexa488/568, goat-anti-rabbit-Alexa488/568/647, goat-anti-mouse-Alexa488/568/647, goat anti-rat-Alexa488 and goat-anti-mouse-IgM-Alexa568 (Invitrogen) diluted to 1:1000 in PBS plus 0.2% Triton X-100.

TUNEL

We used the TUNEL method to detect fragmented DNA in dying cells. We used the *In Situ* Cell Death Kit (TMR red; 1215679910) that was supplied by Roche Applied Science, as per the manufacturer's instructions.

Photography, measurements, cell counts, and statistical analyses

Photomicrographs were obtained using a Leica DM5000B microscope equipped with epifluorescence and Leica DC500 digital camera. Confocal images were obtained using a Zeiss LSM 510 at the Hunt-Curtis Imaging Facility. Images were optimized for color, brightness and contrast, and double-labeled images overlaid by using Adobe Photoshop™ 6.0. Cell counts were made from at least 5 different animals, and means and standard deviations calculated on data sets. To avoid the possibility of region-specific differences within the retina, cell counts were consistently made from the same region of retina for each data set. Images of peripheral retina were taken between 1 and 3 mm from the retinal margin, and images of central retina were taken within 2 mm of the posterior pole of the eye.

Immunofluorescence was quantified by using ImagePro 6.2. Identical illumination, microscope and camera settings were used to obtain images for quantification. Fixed areas were sampled from 5.4 MP digital images. These areas were randomly sampled across all retinal layers or within the inner plexiform layer (IPL). Measurements were made for regions containing pixels with intensity values of 72 or greater (0 = black, 255 = saturated). The total area was calculated for regions with pixel intensities > 72. The average density was calculated as the mean pixel value above threshold within threshold-designated regions. The density sum was calculated as the total of pixel values for all pixels within threshold-designated regions. These calculations were determined for regions sampled from 6 different individuals for each experimental condition.

Results

Through the course of studies into the effects of growth factors upon retinal cells, we identified a novel type of glia-like cell. We distinguished these presumptive glia from other cell types by labeling retinal sections with antibodies to different transcription factors, enzymes and filamentous proteins. Consistent with previous reports (Fischer et al. 2009a; Fischer et al. 2009b), the transcription factor Sox2 was localized to the fusiform nuclei of Müller glia that were stratified in the middle of the INL (Fig. 1a). In addition, Sox2 was found in Islet1^{+} nuclei of cholinergic amacrine cells; these cells were found in the proximal INL and displaced to the ganglion cell layer (GCL; Fig. 1b). Islet1 is also expressed by many horizontal, bipolar and ganglion cells (Fig. 1b), consistent with previous reports (Fischer et al. 2008a)(Fischer et al. 2007; Stanke et al. 2008). In addition, we identified Sox2^{+}/Islet1^{-} cells that were scattered across the IPL, GCL and NFL (Fig. 1b). All (n=813) of the Sox2^{+} cells in the IPL were immunoreactive for Sox9 and transitin (Figs.1c–f, 1h and 1k). Most of these cells were found in the distal third of the IPL, at about 25% IPL depth, and formed fine peripheral processes that tended to extend horizontally within the IPL (Figs. 1f and 1k). Sox9^{+}/Sox2^{+} cells were occasionally observed in the proximal INL, scattered among Sox2^{+} nuclei of cholinergic amacrine cells (Fig. 1i). In addition, all of the nuclei of Müller glia in the middle of the INL were immunoreactive for Sox2 and Sox9 (Fig. 1j). Many of the Sox9^{+} cells in the GCL were not immunoreactive for Sox2 (Figs. 1c–f and 1g).

It was not possible to unambiguously distinguish $Sox9^+$/transitin$^+$ cells in the GCL because of the transitin$^+$ end-feet of Müller glia, which are densely packed within the GCL (not shown). Numbers of $Sox9^+/Sox2^+$ cells in the IPL were more abundant in central regions of the retina compared to dorsal or ventral regions of the retina (Fig. 1l). Similarly, the abundance of $Sox9^+/Sox2^+$ cells was significantly greater in the GCL in central and ventral retina compared to dorsal regions of the retina (Fig. 1m). By comparison, the $Sox9^+/Sox2^-$ cells in the GCL were most abundant in central regions of the retina, with abundance decreasing in ventral and dorsal regions (Fig. 1m).

We next sought to characterize the $Sox9^+/Sox2^-$ cells in the GCL. None of the $Sox9^+/Sox2^-$ cells in the GCL were co-labeled for Brn3a (Supplement Figs. 1h–k); indicating that these cells were not a type of ganglion cell. To test whether the $Sox9^+/Sox2^-$ cells in the GCL were oligodendrocytes we probed for Transferrin Binding Protein (TFBP); a marker that is expressed by oligodendrocytes in the avian central nervous system (Cho and Lucas 1995; Cho et al. 1999; Cho et al. 1997; Won et al. 2000). We found that all (n=387) of the TFBP$^+$ cells in the GCL were immunoreactive for Sox9 (Figs. 2a–c). Most (74.8 ± 8.3%) of the TFBP+ cells were immunoreactive for Nkx2.2 (Figs. 2d–f and Supplemental Figs. 1l–o), whereas few (9.5 ± 4.6%) of the TFBP+ cells were immunoreactive for Sox2 (Supplemental Figs. 1l–o). These findings indicate that many of the $Sox9^+$ cells in the GCL were oligodendrocytes. Interestingly, all (n=328) of the $Sox2^+/Sox9^+$/transitin$^+$ cells in the IPL were positive for Nkx2.2$^+$ (Figs. 2d–i and Supplemental Figs. 1l–o). Further, the Nkx2.2$^+$/TFBP$^-$ cells, indicating non-oliogdendrocytes, in the GCL and NFL were immunoreactive for Sox2 (Figs. 2d–i and Supplemental Figs. 1l–o).

We next tested whether the $Sox9^+/Sox2^+/Nkx2.2^+$/transitin$^+$ cells in the inner retinal layers expressed markers that are normally expressed by glia. Unlike the Müller glia, the $Sox9^+/Sox2^+/Nkx2.2^+$/transitin$^+$ cells in the IPL did not express detectable levels of 2M6 (not shown) or glutamine synthetase (Supplemental Figs. 1a–d). There may have been low levels of Glial Fibrillary Acidic Protein (GFAP) in the $Sox9^+/Sox2^+/Nkx2.2^+$/transitin$^+$ cells, but this was difficult to distinguish because of the high density of GFAP$^+$ processes from Müller glia that wrapped around these cells in the IPL (Supplemental Figs. 1e–g). The $Sox9^+/Sox2^+/Nkx2.2^+$/transitin$^+$ cells were readily distinguished from the astrocytes, which are intensely GFAP-immunoreactive, negative for Sox9 and Sox2, and found distributed sparsely within the GCL (see Fig. 7 for examples). Similar to Müller glia, the $Sox9^+/Sox2^+/Nkx2.2^+$/transitin$^+$ cells in the IPL were immunoreactive for vimentin (Figs. 2j and 2k), suggesting that these cells are glia-like.

We next sought to assess whether the $Sox9^+/Sox2^+/Nkx2.2^+$/transitin+ cells in the inner retinal layers were microglia. Many reports have identified resident, quiescent microglia that are scattered across the IPL of different vertebrates, including the chick (Cuadros et al. 2006; Navascues et al. 1994; Won et al. 2000). Previous reports have suggested that transitin and Sox9 are expressed by cells that are scattered across the IPL in the chick retina; these cells were thought to be quiescent microglia-like cells (Fischer and Omar 2005; Fischer et al. 2009a). However, we found that well-known microglial markers, RCA1 and CD45, were not co-localized to the $Sox2^+/Sox9^+/Nkx2.2^+$/transitin$^+$ cells within the IPL, GCL and NFL. None (n=388) of the RCA1$^+$/CD45$^+$ microglia were labeled for Nkx2.2, Sox9 or transitin (Figs. 2l–o) The markers RCA1 and CD45 are present on all microglia in the avian central nervous system (Cuadros et al. 2006). These findings indicate that the $Sox2^+/Sox9^+/Nkx2.2^+$/transitin$^+$ cells were not microglia.

We believe that the Sox2/Sox9/Nkx2.2/transitin-expressing cells that are scattered within the IPL, GCL and NFL are a novel type of glial cell that is distinct from other types of inner retinal glia, including astrocytes. Accordingly, we have termed these cells Non-astrocytic

Inner Retinal Glia-like (NIRG) cells. The abundance, distribution and phenotype of the NIRG cells did not change significantly during the first 4 weeks of postnatal development. A summary of the immunocytochemical profiles of the different types of retinal glia is provided in table 2.

Effects of IGF1 on retinal cells

Because of recent reports of effects of insulin on the retinal neurons and glia (Fischer et al. 2009a; Punzo et al. 2009) and because insulin can act at IGF1 receptors (Steele-Perkins et al. 1988; Waldbillig et al. 1991), we tested whether intraocular injections of IGF1 influence cells in the chick retina. We began by probing for the expression of receptors to IGF1 and IGF2 by using RT-PCR. We detected mRNA for the IGF1 receptor (IGF1R) and IGF2R in retina and liver, as a positive control (Fig. 3a). Riboprobes to the IGF1R were generated and *in situ* hybridization (ISH) was performed to determine where the receptors were expressed within the retina. Anti-sense riboprobes to IGF1R labeled cells that were scattered across the IPL and GCL, whereas sense probes fail to produce labeling (Figs. 3b and 3c). The only types of cells found within the IPL were NIRG cells or microglia (see Figs. 1, 2 and supplemental Fig. 1). Thus, the NIRG cells and/or microglia are the only types of cells that express detectable levels IGF1R in the postnatal chick retina.

A recent report indicates that insulin stimulates microglia to up-regulate LMG (Fischer et al. 2009a). Thus, we tested whether IGF1 influenced microglia in a manner similar to that of insulin. We found that IGF1-treatment significantly increased immunolabeling for LMG in the IPL (Figs. 3d–e). Both the area and density sum of LMG-immunofluorescence were increased in the IPL of IGF1-treated retinas (Figs. 3f and 3g). To further assess whether microglia are influenced by IGF1 we probed for RCA1 and CD45. Although there was no significant change in the area or density of RCA1-labeling in the IPL in IGF1-treated retinas (not shown), immunolabeling for CD45 was increased in IGF1-treated microglia (Figs. 3h–n). In addition, labeling for CD45 revealed that the morphology of the microglia was altered in IGF1-treated retinas. In control retinas, $CD45^+$ processes were long, thin and widely ramified throughout the IPL (Figs. 3h and 3i). By comparison, IGF1-treated microglia had short, thick peripheral processes that were intensely immunoreactive for CD45 (Figs. 3j and 3k). All of the LMG-immunoreactive puncta in IGF1-treated retinas were co-localized to $CD45^+$ microglia (Figs. 3l–n). Microglia are known to proliferate and up-regulate LMG in response to acute retinal damage (Fischer and Reh 2001; Fischer et al. 1998). However, there was no evidence that IGF1-treatment caused retinal damage. We failed to find cells that were labeled for cleaved caspase 3 or TUNEL in IGF1-treated retinas (not shown).

We assayed for the effects of IGF1 on retinal cells by probing for cellular proliferation and phosphorylation of components of the MAPK-signaling pathways. Although IGF1 is best known to signal through phosphatidylinositol 3 kinase (PI3K)/Akt in neural tissue, IGF1 can also signal through branches of the MAPK pathway (reviewed by Aberg and colleagues, 2006). Control retinas contained p38 MAPK-immunoreactivity at low levels in Müller glia (Figs. 4a and 4c), consistent with a previous report (Fischer et al. 2009a). Levels of p38 MAPK were significantly increased in Müller glia in central and peripheral regions of the retina in response to injections of IGF1 (Figs. 4a–d). All (n=302) of the $Sox2^+$ Müller glia were immunoreactive for p38 MAPK (Figs. 4e–g). In addition, IGF1-treatment stimulated the up-regulation of cFos in many Müller glia (Figs. 4h–k). More than half (54.3 ± 6.4%) of the $Sox2^+$ Müller glia expressed cFos in IGF1-treated retinas. Furthermore, levels of GFAP were increased in Müller glia treated with IGF1, whereas levels of GFAP appeared unaffected by injections of vehicle (Figs. 4l–o). There were no significant increases in labeling for pERK, Egr1 or pCREB in IGF1-treated retinas (not shown). IGF1 did not influence the distribution or morphology of oligodendrocytes that were labeled for TBFP,

Sox9 and Nkx2.2 (not shown). Injections of IGF2 did not influence levels of pERK1/2, pCREB, p38 MAPK, cFos or Egr1 in Müller glia or neurons in the retina (not shown).

NIRG cells are stimulated by IGF1

IGF1 stimulated a dramatic increase in transitin-immunoreactive processes that permeated the IPL, whereas levels of transitin-immunofluoresence in saline-treated IPL were low (Figs. 5a-f). Quantitative immunofluoresence indicated a significant increase in the area and density of transitin-labeling in the IPL of IGF1-treated retinas (Figs. 5c–f). The thick transitin-immunoreactive processes that accumulated in the IPL of IGF1-treated retinas were those of $Sox2^+/Sox9^+$ NIRG cells (Figs. 5b and 5j). In addition, IGF1-treatment appeared to modestly increase transitin-immunoreactivity in Müller glia (Figs. 5a and 5b). Identical results were obtained with 2 different monoclonal antibodies to transitin (not shown).

IGF1-treatment caused a redistribution of $Sox2^+/Sox9^+/Nkx2.2^+$ cells within the IPL, GCL and NFL (Figs. 5g–k). In control retinas, most of the $Sox2^+/Sox9^+/Nkx2.2^+$ cells were found in the GCL and NFL (Figs. 5g–k). In IGF1-treated retinas, numbers of $Sox2^+/Sox9^+/Nkx2.2^+$ cells were increased in the IPL and decreased in the GCL/NFL compared to numbers observed in vehicle-treated retinas (Figs. 5g–k). These findings suggest that the NIRG cells migrate distally into the retina in response to IGF1. In addition, there was a significant increase in the number of $Sox2^+$ Müller glial nuclei that were displaced away from the center of the INL in IGF1-treated retinas (Figs. 5a,b,g and h). Intraocular injections of IGF2 did not appear to influence the NIRG cells or Müller glia (not shown).

We next tested whether IGF1 stimulated NIRG cells to adopt phenotypes of reactive microglia or remain as a distinct type of cell. In IGF1-treated retinas, none (n=349) of the $Sox9^+$/transitin$^+$ cells in the IPL were labeled for RCA1 (Supplemental Figs. 2a–e) or CD45 (not shown). Conversely, none (n=289) of the $RCA1^+$ microglia were co-labeled for Sox9 or transitin (Supplemental Figs. 2a–c). These findings indicate that the NIRG cells and the microglia remain as distinctly different cell types when stimulated by IGF1 to acquire “reactive” phenotypes. In addition, the NIRG cells accumulated p38 MAPK in response to IGF1, whereas the $RCA1^+$ microglia did not (Supplemental Figs. 2c–e).

We tested whether the accumulation of cells in the IPL in IGF1-treated retinas resulted from proliferation. Very few BrdU-labeled cells (one or two cells per section) were observed in control retinas (not shown). By contrast, numerous BrdU-labeled cells (57.3 ± 14.1 cells per section) were observed in retinas treated with IGF1 (Figs. 5l–n). These cells were found scattered across central and peripheral regions of the retina, and were found in the NFL, GCL or IPL (Figs. 5l–p). The majority of BrdU-labeled cells (70.1 ± 11.0%; n=285 cells) in the IPL, GCL or NFL were $Sox2^+$ (Figs. 5l–n), and the remaining BrdU-labeled cells were RCA1+ microglia (not shown). More than half (61.9 ± 8.6%; n= 461) of the $Sox2^+$ cells in the IPL were labeled for BrdU, suggesting that many of the $Sox2^+$ cells that migrated into the IPL were newly generated.

IGF1-treatment exacerbates the damage that results from NMDA-induced excitotoxicity

We have reported previously that insulin-treatment before NMDA increases numbers of dying retinal neurons (Fischer et al. 2009a). Accordingly, we tested whether injections of IGF1 influenced NMDA-induced retinal damage. There was a dramatic increase in retinal detachments in all retinas (n=14) treated with IGF1 before NMDA (Figs. 6a–e). The detachments appeared as opaque wrinkles scattered across all regions of the retina (Figs. 6a–c). In vertical sections through the retina, detachments between the Retinal Pigmented Epithelium (RPE) and photoreceptors were as large as 180 μm (Figs. 6d and 6e).

We assayed for cell death by using the TUNEL method to label fragmented DNA *in situ*. In retinas treated with NMDA alone, we found $TUNEL^+$ nuclei scattered across the INL (Fig. 6f), consistent with previous reports (Fischer et al. 2004;Fischer et al. 1998). By comparison, significantly more $TUNEL^+$ cells were observed in NMDA-damaged retinas that were pre-treated with IGF1. In non-detached regions of IGF1 pre-treated retinas, numbers of $TUNEL^+$ cells in the INL were not significantly different from numbers observed in retinas treated with NMDA alone (Figs. 6f–h). By contrast, numbers of $TUNEL^+$ cells were increased nearly four-fold in regions of retinal detachment (Figs. 6f–h). In detached regions of retina $TUNEL^+$ cells were found in the outer nuclear layer (ONL; Fig. 6g), suggesting the death of photoreceptors. IGF2 had no effect upon the levels of death resulting from NMDA-treatment (not shown).

We probed for different glial markers to better characterize the effects of IGF1-treatment prior to an excitotoxic insult. One day after treatment with NMDA alone we found few NIRG cells in the IPL and relatively low levels of transitin-immunoreactivity in the NIRG cells and Müller glia (Fig. 7a). In retinas treated with IGF1 before NMDA, increased numbers of NIRG cells accumulated in the IPL and levels of transitin-immunoreactivity were elevated in both NIRG cells and Müller glial processes (Fig. 7b). Interestingly, there was a stark absence of Müller glia in detached regions of retina. In detached regions there was an absence of vertically oriented Müller glial processes that where immunoreactive for GFAP, transitin (Figs. 7c–f), vimentin (Figs. 7m–q and 7v–y), 2M6 (Figs. 7r–u), and glutamine synthetase (not shown). In detached regions, Müller glial nuclei labeled for Sox2 and Sox9 were missing from the INL (Figs. 7c–e and 7r–u). NIRG cells accumulated within the IPL in areas of detachment (Figs. 7c–f and 7m–y). Within adherent and detached regions of retina, the NIRG cells were weakly immunoreactive for GFAP, unlike the surviving Müller glia and sparsely distributed astrocytes which were intensely immunoreactive for GFAP (Figs. 7c–l). The astrocytes remained within the GCL or NFL and were negative for Sox2 (Figs. 7g–l) and Sox9 (not shown). Within the IPL of detached regions of retina, the NIRG cells formed thick peripheral processes that were intensely immunoreactive for transitin (Figs. 7c–f) and vimentin (Figs. 7m–q and 7v–y). The NIRG cells in regions of detached retina were distinguished from de-laminated, reactive Müller glia by labeling for Nkx2.2 (Figs. 7v–y). Furthermore, the NIRG cells did not express Pax6 in damaged retinas (results not shown), unlike Müller glia which are known to express Pax6 following NMDA-treatment (Fischer et al. 2002;Fischer and Reh 2001).

Three days after treatment with IGF1/NMDA, detached areas of retina remained as opaque spots on the retina (Figs. 8a–d). Compared to retinas treated with NMDA alone, retinas pretreated with IGF1 contained elevated levels of $TUNEL^+$ cells in adherent and detached regions (Figs. 8e–g). In detached retinal regions there were numerous $TUNEL^+$ cells in the ONL, unlike adherent regions where $TUNEL^+$ cells were confined to the INL (Figs. 8e and 8g). In detached areas, there were no Müller glia labeled for 2M6 or glutamine synthetase (Figs. 8h–j), whereas there was an accumulation of $Sox9^+/Sox2^+/transitin^+$ NIRG cells (Figs. 8h–m). In addition, few $GFAP^+$ processes, co-labeled for transitin, were found within the inner layers of detached retinal regions (Figs. 8k–m); these processes likely were those of NIRG cells.

There were increased numbers of proliferating microglia and NIRG cells in retinas treated with IGF1 before NMDA. The proliferating cells were labeled for Proliferating-Cell Nuclear Antigen (PCNA) and BrdU, and were found within the IPL of NMDA-damaged retinas that were pre-treated with IGF1 (supplemental Figs. 3a–c and 3i–n). Approximately one-third (30.3 ± 8.9%) of the proliferating cells in the IPL were LMG^+ microglia (supplemental Figs. 3d–f). The remainder of the proliferating cells in the IPL were $Sox2^+$ NIRG cells (supplemental Figs. 3g and 3h).

Discussion

We report here that a novel type of cell, that we termed the Non-astrocytic Inner Retinal Glia-like (NIRG) cell, is normally found scattered within the IPL, GCL and NFL. The NIRG cells share phenotypic similarities to Müller glia and retinal progenitors. We find that IGF1 has profound affects upon retinal glia and neuronal survival following excitotoxic stress. IGF1 stimulated Müller glia to up-regulate p38 MAPK and cFos, whereas microglia up-regulate LMG and CD45. In addition, IGF1 stimulated the migration of NIRG cells distally into the retina and this was coincident with proliferation and increased transitin expression. Coincident with these changes in glial activity, retinal neurons are rendered more susceptible to an excitotoxic insult. Since microglia and NIRG cells are the only types of cells found within the IPL, and the IGF1 receptor was detected only in the IPL, we conclude that the effects of IGF1 are manifested through the NIRG cells and/or microglia in the postnatal chick retina.

The NIRG cells have phenotypic similarities with retinal progenitors. These similarities include the ability to proliferate, expression of the filamentous proteins transitin and vimentin, and expression of the transcription factors Sox2 and Sox9. In the retina, the Müller glia and progenitors share significant overlap in their transcriptomes; more than two-thirds of the genes expressed by Müller glia are also expressed by progenitors (Jadhav et al. 2009; Roesch et al. 2008). Therefore, it is not surprising that retinal glia can de-differentiate to produce proliferating neural progenitors; this has been demonstrated in different vertebrate species (Bernardos et al. 2007; Fausett and Goldman 2006; Fischer and Reh 2001; Karl et al. 2008). In the chick retina, for example, in response to acute neuronal damage numerous Müller glia de-differentiate, re-enter the cell-cycle, and express genes normally found in embryonic retinal progenitors. These genes include CASH1 (ascl1a), Pax6, Chx10, PCNA (Fischer and Reh 2001), Six3 (Fischer 2005), Notch1, Sox2 (Hayes et al. 2007), Sox9 (Fischer et al. 2009a) and transitin (Fischer and Omar 2005). Although the NIRG cells express many genes that are found in retinal stem cells and Müller glia-derived progenitors, the potential of the NIRG cells to act as neural progenitors remains untested. The neurogenic potential of NIRG cells remains a distinct possibility given that these cells express Sox2, Sox9, PCNA (when stimulated by IGF1) and transitin, similar to retinal progenitors. However, in the current study we did not detect Pax6 in the NIRG cells; Pax6 is a transcription factor that is crucial to the normal function of retinal progenitors (reviewed by Marquardt 2003). Further, the NIRG cells expressed Nkx2.2, a homeodomain transcription factor expressed by precursors of dopaminergic neurons in the ventral midbrain (Prakash and Wurst 2007), medial longitudinal fascicle (Ahsan et al. 2007), serotonergic neurons in the raphe nucleus in the brain stem (Alenina et al. 2006) and by oligodendrocyte precursors in the developing spinal cord (Qi et al. 2001; Soula et al. 2001; Zhou et al. 2001). The $Nkx2.2^{+}$ NIRG cells in the chick retina, clearly, were not dopaminergic or serotonergic amacrine cells, and the NIRG cells were distinguished from oligodendrocytes. To the best of our knowledge, there are currently no reports of $Nkx2.2^{+}$ cells in the vertebrate retina.

The NIRG cells appear to be a type of glial cell. Similar to Müller glia, the NIRG cells express vimentin, transitin, Sox2 and Sox9, accumulate p38 MAPK, and migrate distally into the retina in response to intraocular injections of IGF1. In addition, both the Müller glia and NIRG cells re-enter the cell cycle in response to acute retinal damage. Unlike Müller glia, the NIRG cells express Nkx2.2, low levels of GFAP and do not express 2M6, glutamine synthetase, or Pax6. However, it is possible that some of these glial/progenitor markers are expressed by the NIRG cells during earlier stages of differentiation. For example, Prada and colleagues have reported that during late stages of chick embryonic development, astrocyte-like cells located in the GCL express glutamine synthetase (Prada et al. 1998). However, the existence of astrocytes in the chick retina remains controversial

(Won et al. 2000). Nevertheless, we find cells in the chick retina that strongly resemble astrocytes, and these cells are distinctly different from NIRG cells. The presumptive astrocytes are sparsely distributed among the ganglion cells, express high levels of GFAP, do not express Sox2 or Sox9, and appear to have an astrocyte-like morphology (see Fig. 7 for examples). We cannot exclude the possibility that the NIRG cells are some type of transitional glial cell. However, this seems unlikely given that NIRG cells are found in normal, undamaged retina, and the phenotype and distribution of these cells appears unchanged during the first 4 weeks postnatal development.

The NIRG cells have not been previously described and distinguished from other types of retinal glia. We have reported that microglia-like cells are scattered across the IPL and GCL, and these cells are immunoreactive for transitin, Sox9 and p38 MAPK (Fischer et al. 2009a). We mistakenly assumed, based on morphology, distribution and location within the retina, that the transitin/Sox9/p38MAPK$^+$ cells were microglia. In the current study we provide unambiguous evidence that the transitin/Sox2/Sox9/p38MAPK$^+$ cells are not microglia. Accordingly, the transitin/Sox2/Sox9/p38MAPK$^+$ cells appear to be Non-astrocytic Inner Retinal Glia–like (NIRG) cells. The function of the NIRG cells in the normal, healthy retina remains uncertain. However, given the sparse distribution and location of the NIRG cells, we speculate that the normal activity of the cells may be to maintain synaptic function within the IPL and/or provide support to ganglion cells.

The effects of insulin and IGF1 upon retinal glia are significantly different. In prior studies, insulin stimulated Müller glia to accumulate cFos and Egr1, but not p38 MAPK (Fischer et al. 2009a). By comparison, we report here that IGF1 stimulates Müller glia to accumulate p38 MAPK and express cFos, in a random pattern, but not Egr1. Both insulin and IGF1 cause the accumulation of LMG in microglia, up-regulation of transitin in NIRG cells, and increase levels of cell death in response to NMDA-treatment (current study and (Fischer et al. 2009a). Unlike IGF1, insulin-treatment before NMDA does not cause retinal folds and detachments associated with losses of Müller glia. Interestingly, insulin receptors are not expressed in the chick retina (Fischer et al. 2009a). Thus, some of the effects of insulin may be elicited through IGF1 receptors, but the differences between the effects of insulin and IGF1 may result from the activation of receptors in addition to IGF1R. Alternatively, binding of insulin to IGF1R may activate different cell signaling pathways than those activated by IGF1. For example, different ligands that bind the same receptor can recruit different second messengers and elicit different cellular responses (Bohn 2007; Raehal and Bohn 2005)

IGF1 is known to promote the survival of neurons during early stages of brain development (reviewed by Bondy and Cheng 2004). In the developing retina, insulin and IGF1 promote the survival of neurons (de la Rosa and de Pablo 2000; Varela-Nieto et al. 2003; Vecino et al. 2004). However, in the mature nervous system insulin/IGF1 can attenuate the survival of neurons (reviewed by Cohen and Dillin 2008). In the mature retina, a recent report indicates that insulin supports the survival of cone photoreceptors amidst degeneration of the rods in a model of retinitis pigmentosa (Punzo et al. 2009). Here we show that IGF1 increases the susceptibility of Müller glia and retinal neurons to excitotoxic damage. Taken together, these findings indicate that the effects of insulin and IGF1 upon the survival of neurons are different between the mature and developing retina, and perhaps between retinal cell types. The primary effects of insulin and IGF1 may be manifested through the NIRG cells and microglia, whereas neurons and Müller glia may be indirectly affected. We find that the IGF1 receptor is expressed by cells scattered within the IPL and GCL, and not by cells in other retinal layers. The expression pattern of the IGF1 receptor is consistent with the distribution of NIRG cells and microglia. Thus, the effects of IGF1 on Müller glia and the susceptibility of neurons to damage may be secondary to activation of IGF1 receptors on

NIRG cells and/or microglia. We cannot exclude the possibility that IGF1 is acting at retinal cells in addition to the NIRG cells and microglia, perhaps through IGF2 receptors, to influence the susceptibility of neurons to damage.

Conclusions

We provide evidence for a novel type of glial cell that is normally scattered across inner layers of the retina. These cells are distinctly different from retinal astrocytes, microglia, oliogdendrocytes and Müller glia, but share some phenotypic similarities with Müller glia and retinal progenitors. These NIRG cells are stimulated by IGF1 to proliferate, up-regulate the filamentous protein transitin, and migrate distally into the retina. In addition, IGF1 caused microglia to acquire a reactive phenotype. With the microglia and NIRG cells stimulated by IGF1, retinal neurons and Müller glia were rendered more susceptible to an excitotoxic insult. We propose that the interactions of the different types of glial cells within the retina are crucial to supporting the survival of neurons under condition of stress.

Supplementary Material

Refer to Web version on PubMed Central for supplementary material.

Acknowledgments

We thank Drs. Paul Henion and Paul Linser for providing antibodies to transitin and 2M6, respectively. Confocal microscopy was performed at the Hunt-Curtis Imaging Facility at the Department of Neuroscience of The Ohio State University. The BrdU, LEP100, Pax6, Nkx2.2 and transitin antibodies developed by Drs S.J. Kaufman, D.M. Fambrough, A. Kawakami, T.M. Jessell and G.J. Cole, respectively, were obtained from the Developmental Studies Hybridoma Bank developed under auspices of the NICHD and maintained by the University of Iowa, Department of Biological Sciences, Iowa City, IA 52242. This work was supported by a grant (EY016043) from the National Institutes of Health.

References

Ahsan M, Riley KL, Schubert FR. Molecular mechanisms in the formation of the medial longitudinal fascicle. J Anat. 2007; 211(2):177–87. [PubMed: 17623036]

Alenina N, Bashammakh S, Bader M. Specification and differentiation of serotonergic neurons. Stem Cell Rev. 2006; 2(1):5–10. [PubMed: 17142880]

Barres BA, Raff MC. Proliferation of oligodendrocyte precursor cells depends on electrical activity in axons. Nature. 1993; 361(6409):258–60. [PubMed: 8093806]

Barres BA, Raff MC. Axonal control of oligodendrocyte development. J Cell Biol. 1999; 147(6): 1123–8. [PubMed: 10601327]

Bernardos RL, Barthel LK, Meyers JR, Raymond PA. Late-stage neuronal progenitors in the retina are radial Muller glia that function as retinal stem cells. J Neurosci. 2007; 27(26):7028–40. [PubMed: 17596452]

Bohn LM. Constitutive trafficking--more than just running in circles? Mol Pharmacol. 2007; 71(4): 957–8. [PubMed: 17251327]

Bondy CA, Cheng CM. Signaling by insulin-like growth factor 1 in brain. Eur J Pharmacol. 2004; 490(1–3):25–31. [PubMed: 15094071]

Bringmann A, Pannicke T, Grosche J, Francke M, Wiedemann P, Skatchkov SN, Osborne NN, Reichenbach A. Muller cells in the healthy and diseased retina. Prog Retin Eye Res. 2006; 25(4): 397–424. [PubMed: 16839797]

Bringmann A, Reichenbach A. Role of Muller cells in retinal degenerations. Front Biosci. 2001; 6:E72–92. [PubMed: 11578954]

Cho SS, Lucas JJ. Immunocytochemical study with an anti-transferrin binding protein serum: a marker for avian oligodendrocytes. Brain Res. 1995; 674(1):15–25. [PubMed: 7773685]

Cho SS, Lucas JJ, Hyndman AG. Transferrin binding protein is expressed by oligodendrocytes in the avian retina. Brain Res. 1999; 816(1):229–33. [PubMed: 9878753]

Cho SS, Lucas JJ, Roh EJ, Yoo YB, Lee KH, Park KH, Hwang DH, Baik SH. Distribution of transferrin binding protein immunoreactivity in the chicken central and peripheral nervous systems. J Comp Neurol. 1997; 382(2):260–71. [PubMed: 9183693]

Cohen E, Dillin A. The insulin paradox: aging, proteotoxicity and neurodegeneration. Nat Rev Neurosci. 2008; 9(10):759–67. [PubMed: 18769445]

Cuadros MA, Santos AM, Martin-Oliva D, Calvente R, Tassi M, Marin-Teva JL, Navascues J. Specific immunolabeling of brain macrophages and microglial cells in the developing and mature chick central nervous system. J Histochem Cytochem. 2006; 54(6):727–38. [PubMed: 16461367]

de la Rosa EJ, de Pablo F. Cell death in early neural development: beyond the neurotrophic theory. Trends Neurosci. 2000; 23(10):454–8. [PubMed: 11006461]

Fausett BV, Goldman D. A role for alpha1 tubulin-expressing Muller glia in regeneration of the injured zebrafish retina. J Neurosci. 2006; 26(23):6303–13. [PubMed: 16763038]

Fischer AJ. Neural regeneration in the chick retina. Prog Retin Eye Res. 2005; 24(2):161–82. [PubMed: 15610972]

Fischer AJ, Foster S, Scott MA, Sherwood P. Transient expression of LIM-domain transcription factors is coincident with delayed maturation of photoreceptors in the chicken retina. J Comp Neurol. 2008a; 506(4):584–603. [PubMed: 18072193]

Fischer AJ, McGuire CR, Dierks BD, Reh TA. Insulin and fibroblast growth factor 2 activate a neurogenic program in Muller glia of the chicken retina. J Neurosci. 2002; 22(21):9387–98. [PubMed: 12417664]

Fischer AJ, McGuire JJ, Schaeffel F, Stell WK. Light- and focus-dependent expression of the transcription factor ZENK in the chick retina. Nat Neurosci. 1999; 2(8):706–12. [PubMed: 10412059]

Fischer AJ, Omar G. Transitin, a nestin-related intermediate filament, is expressed by neural progenitors and can be induced in Muller glia in the chicken retina. J Comp Neurol. 2005; 484(1): 1–14. [PubMed: 15717308]

Fischer AJ, Reh TA. Muller glia are a potential source of neural regeneration in the postnatal chicken retina. Nat Neurosci. 2001; 4(3):247–52. [PubMed: 11224540]

Fischer AJ, Ritchey ER, Scott MA, Wynne A. Bullwhip neurons in the retina regulate the size and shape of the eye. Dev Biol. 2008b; 317(1):196–212. [PubMed: 18358467]

Fischer AJ, Schmidt M, Omar G, Reh TA. BMP4 and CNTF are neuroprotective and suppress damage-induced proliferation of Muller glia in the retina. Mol Cell Neurosci. 2004; 27(4):531–42. [PubMed: 15555930]

Fischer AJ, Scott MA, Ritchey ER, Sherwood P. Mitogen-activated protein kinase-signaling regulates the ability of Muller glia to proliferate and protect retinal neurons against excitotoxicity. Glia. 2009a; 57(14):1538–52. [PubMed: 19306360]

Fischer AJ, Scott MA, Tuten W. Mitogen-activated protein kinase-signaling stimulates Muller glia to proliferate in acutely damaged chicken retina. Glia. 2009b; 57(2):166–81. [PubMed: 18709648]

Fischer AJ, Seltner RL, Poon J, Stell WK. Immunocytochemical characterization of quisqualic acid- and N-methyl-D-aspartate-induced excitotoxicity in the retina of chicks. J Comp Neurol. 1998; 393(1):1–15. [PubMed: 9520096]

Fischer AJ, Skorupa D, Schonberg DL, Walton NA. Characterization of glucagon-expressing neurons in the chicken retina. J Comp Neurol. 2006; 496(4):479–94. [PubMed: 16572462]

Fischer AJ, Stanke JJ, Aloisio G, Hoy H, Stell WK. Heterogeneity of horizontal cells in the chicken retina. J Comp Neurol. 2007; 500(6):1154–71. [PubMed: 17183536]

Friedlander M, Dorrell MI, Ritter MR, Marchetti V, Moreno SK, El-Kalay M, Bird AC, Banin E, Aguilar E. Progenitor cells and retinal angiogenesis. Angiogenesis. 2007; 10(2):89–101. [PubMed: 17372851]

Giaume C, Kirchhoff F, Matute C, Reichenbach A, Verkhratsky A. Glia: the fulcrum of brain diseases. Cell Death Differ. 2007; 14(7):1324–35. [PubMed: 17431421]

Hayes S, Nelson BR, Buckingham B, Reh TA. Notch signaling regulates regeneration in the avian retina. Dev Biol. 2007; 312(1):300–11. [PubMed: 18028900]

Jadhav AP, Roesch K, Cepko CL. Development and neurogenic potential of Muller glial cells in the vertebrate retina. Prog Retin Eye Res. 2009; 28(4):249–62. [PubMed: 19465144]

Karl MO, Hayes S, Nelson BR, Tan K, Buckingham B, Reh TA. Stimulation of neural regeneration in the mouse retina. Proc Natl Acad Sci U S A. 2008; 105(49):19508–13. [PubMed: 19033471]

Marquardt T. Transcriptional control of neuronal diversification in the retina. Prog Retin Eye Res. 2003; 22(5):567–77. [PubMed: 12892642]

Navascues J, Moujahid A, Quesada A, Cuadros MA. Microglia in the avian retina: immunocytochemical demonstration in the adult quail. J Comp Neurol. 1994; 350(2):171–86. [PubMed: 7884036]

Prada FA, Quesada A, Dorado ME, Chmielewski C, Prada C. Glutamine synthetase (GS) activity and spatial and temporal patterns of GS expression in the developing chick retina: relationship with synaptogenesis in the outer plexiform layer. Glia. 1998; 22(3):221–36. [PubMed: 9482209]

Prakash N, Wurst W. A Wnt signal regulates stem cell fate and differentiation in vivo. Neurodegener Dis. 2007; 4(4):333–8. [PubMed: 17627138]

Punzo C, Kornacker K, Cepko CL. Stimulation of the insulin/mTOR pathway delays cone death in a mouse model of retinitis pigmentosa. Nat Neurosci. 2009; 12(1):44–52. [PubMed: 19060896]

Qi Y, Cai J, Wu Y, Wu R, Lee J, Fu H, Rao M, Sussel L, Rubenstein J, Qiu M. Control of oligodendrocyte differentiation by the Nkx2.2 homeodomain transcription factor. Development. 2001; 128(14):2723–33. [PubMed: 11526078]

Raehal KM, Bohn LM. Mu opioid receptor regulation and opiate responsiveness. Aaps J. 2005; 7(3):E587–91. [PubMed: 16353937]

Roesch K, Jadhav AP, Trimarchi JM, Stadler MB, Roska B, Sun BB, Cepko CL. The transcriptome of retinal Muller glial cells. J Comp Neurol. 2008; 509(2):225–38. [PubMed: 18465787]

Soula C, Danesin C, Kan P, Grob M, Poncet C, Cochard P. Distinct sites of origin of oligodendrocytes and somatic motoneurons in the chick spinal cord: oligodendrocytes arise from Nkx2.2-expressing progenitors by a Shh-dependent mechanism. Development. 2001; 128(8):1369–79. [PubMed: 11262237]

Stanke JJ, Lehman B, Fischer AJ. Muscarinic signaling influences the patterning and phenotype of cholinergic amacrine cells in the developing chick retina. BMC Dev Biol. 2008; 8(1):13. [PubMed: 18254959]

Steele-Perkins G, Turner J, Edman JC, Hari J, Pierce SB, Stover C, Rutter WJ, Roth RA. Expression and characterization of a functional human insulin-like growth factor I receptor. J Biol Chem. 1988; 263(23):11486–92. [PubMed: 2969892]

Tsai HH, Miller RH. Glial cell migration directed by axon guidance cues. Trends Neurosci. 2002; 25(4):173–5. discussion 175–6. [PubMed: 11998681]

Varela-Nieto I, de la Rosa EJ, Valenciano AI, Leon Y. Cell death in the nervous system: lessons from insulin and insulin-like growth factors. Mol Neurobiol. 2003; 28(1):23–50. [PubMed: 14514984]

Vecino E, Hernandez M, Garcia M. Cell death in the developing vertebrate retina. Int J Dev Biol. 2004; 48(8–9):965–74. [PubMed: 15558487]

Waldbillig RJ, Arnold DR, Fletcher RT, Chader GJ. Insulin and IGF-I binding in developing chick neural retina and pigment epithelium: a characterization of binding and structural differences. Exp Eye Res. 1991; 53(1):13–22. [PubMed: 1879497]

Won MH, Kang TC, Cho SS. Glial cells in the bird retina: immunochemical detection. Microsc Res Tech. 2000; 50(2):151–60. [PubMed: 10891879]

Zhou Q, Choi G, Anderson DJ. The bHLH transcription factor Olig2 promotes oligodendrocyte differentiation in collaboration with Nkx2.2. Neuron. 2001; 31(5):791–807. [PubMed: 11567617]

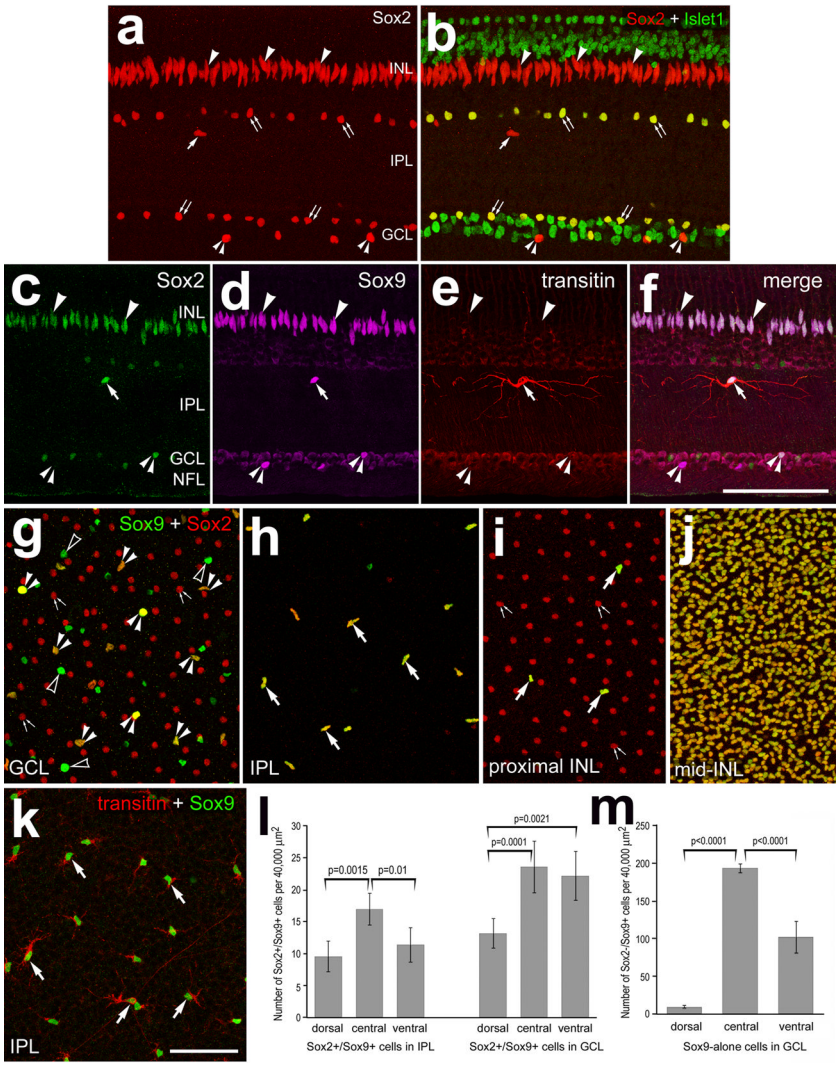

Figure 1.

Glia-like cells that express Sox2, Sox9 and transitin are scattered across the IPL and GCL. Retinas were obtained from untreated eyes. Vertical sections (**a–f**) and flat-mounts (**g–k**) of the retina were labeled with antibodies to Sox2 (red in **a**, **b** and **g–j**; green in **c** and **f**), Islet1 (green in **b**), Sox9 (magenta in **d** and **f**; green in **g–k**), and transitin (red in **e**, **f** and **k**). Confocal microscopy was used to obtain Z-stacks of optical sections. Between 4 and 12 optical sections were projected through the GCL (**g**), IPL (**h**), proximal INL (**i** and **k**) and mid-INL (**j**). Arrows indicate the nuclei of NIRG cells in the IPL (**a–f**, **h** and **k**) and proximal INL (**i**). Small double arrow-heads indicate putative NIRG cells ($Sox9^+/Sox2^+$) in the GCL (**a–g**). Arrow-heads indicate the nuclei of Müller glia (**a–f**). Small double-arrows indicate $Sox2^+$ nuclei of cholinergic amacrine cells (**a**,**b**,**g** and **i**). The calibration bar (50 µm) in panel **f** applies to **a–f**, and the bar in **k** applies to **g–k**. Panel **l** is a histogram illustrating the average number of Sox2+/Sox9+ cells per 40,000 μm^2 in the IPL or GCL for dorsal, central and ventral regions of the retina. Panel **m** is a histogram illustrating the average number of Sox2-/Sox9+ (Sox9 alone) cells per 40,000 μm^2 in the GCL for dorsal, central and ventral regions of the retina.

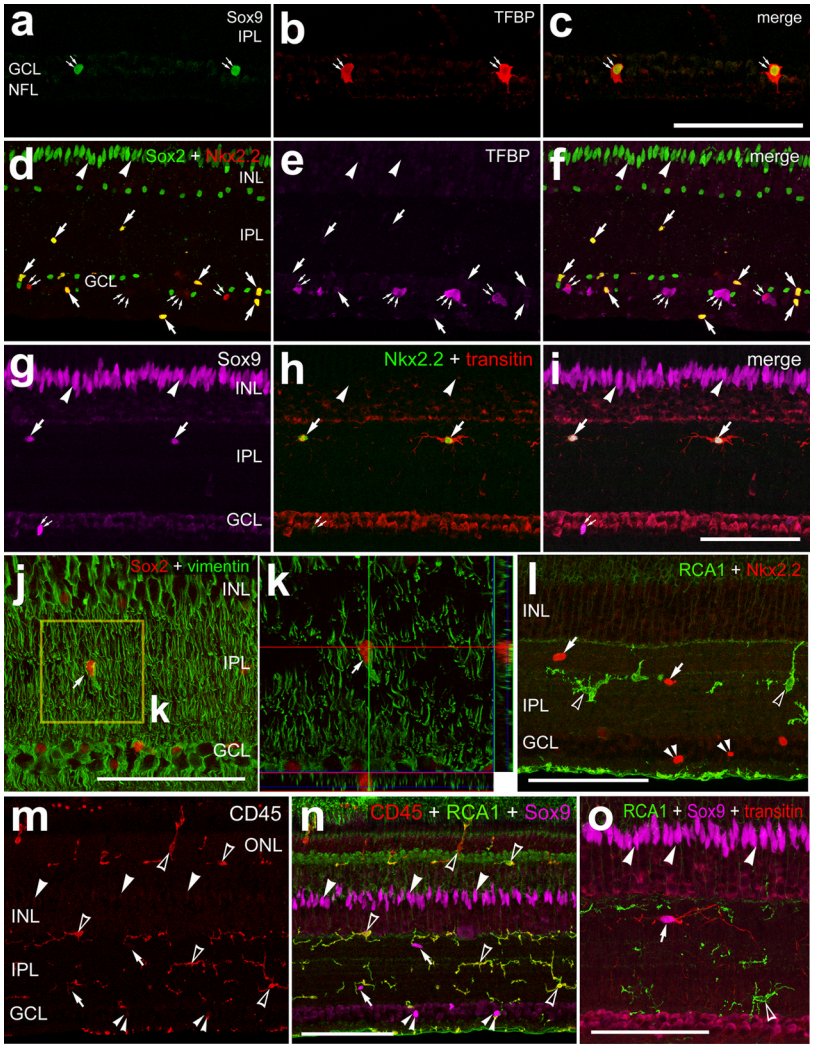

Figure 2.

NIRG cells express Nkx2.2 and vimentin, and are distinctly different from microglia and oligodendrocytes. Retinas were obtained from untreated eyes. Vertical sections of the retina were labeled with antibodies to Sox9 (green in **a** and **c**; magenta in **g**,**I**,**n** and **o**), TBFP (red in **o** and **p**; magenta in **e** and **f**), Sox2 (green in **d** and **f**; red in **j** and **k**), Nkx2.2 (red in **d**,**f** and **l**), transitin (red in **e**,**f** and **o**), vimentin (green in **j** and **k**), and CD45 (red in **m** and **n**), or labeled with biotinylated RCA1 (green in **l**,**k** and **o**). Z-stacks of optical sections were obtained using confocal microscopy. Images were created for maximum intensity projections of 4–6 optical sections or an orthogonal reconstruction (**h** alone). Arrows indicated NIRG cells, arrow-heads indicate the nuclei of Müller glia, small double-arrows indicate Nkx2.2+ oligodendrocytes, small triple-arrows indicate Nkx2.2− oligodendrocytes, small double-arrow-heads indicate $Sox9^{+}$/$Nkx2.2^{+}$ cells in the GCL, and hollow arrow-heads indicate microglia. The scale bar (50 μm) in panel **a** applies to panels **a–c** and, the bar in **I** applies to **d–I**, the bar in **g** applies to **g** alone, the bar in **l** applies to **l** alone, the bar in **n** applies to **m** and **n**, and the bar in **o** applies to **o** alone.

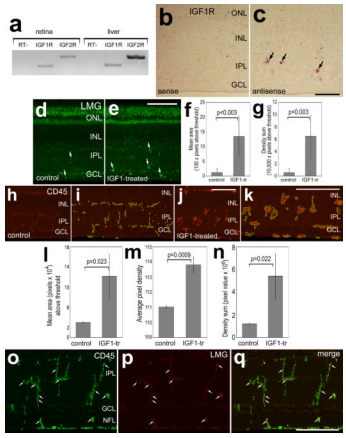

Figure 3.

The IGF1 receptor is expressed by retinal cells that are scattered across inner retinal layers and IGF1 stimulates microglia to up-regulation of LMG and CD45. RT-PCR was used to detect IGF1R and IGF2R in the retina and liver (**a**). *In situ* hybridization was used with sense (**b**) and antisense (**c**) riboprobes to detect mRNA for IGF1R in retinal sections. Retinas were obtained from eyes that were un-injected (**b** and **c**), or received 2 consecutive daily injections of vehicle (**d**,**h** and **i**) or 800 ng IGF1 (**e**,**j**,**k** and **o–p**). Vertical sections of the retina were immunolabeled for LMG (green in **d** and **e**; red in **p** and **q**) and CD45 (**h–k**, **o** and **q**). ImagePro 6.2 was used measure total areas for pixel intensities >72 for LMG and CD45 (0 = black, 255 = saturated), and the density sum (total of pixel values within thresholded objects). Measurements of LMG were made for fixed areas sampled within the IPL, whereas measurements of CD45 included all retinal layers. The green outlines in panels **i** and **k** indicate the areas designed by ImagePro 6.2 for each object that met the threshold criteria. Small arrows indicate microglia that are immunoreactive for LMG and/or CD45. Histograms illustrate means (n=6) and standard deviations. Significance of difference (p-values) was determined by using a two-tailed, unpaired Student's t-test. The scale bar (50 μm) in panel **c** applies to panels **b** and **c**, the bar in **e** applies to **d** and **e**, the bar in **j** applies to **h** and **j**, the bar in **k** applies to **i** and **k**, and the bar in **q** applies to **o–q**.

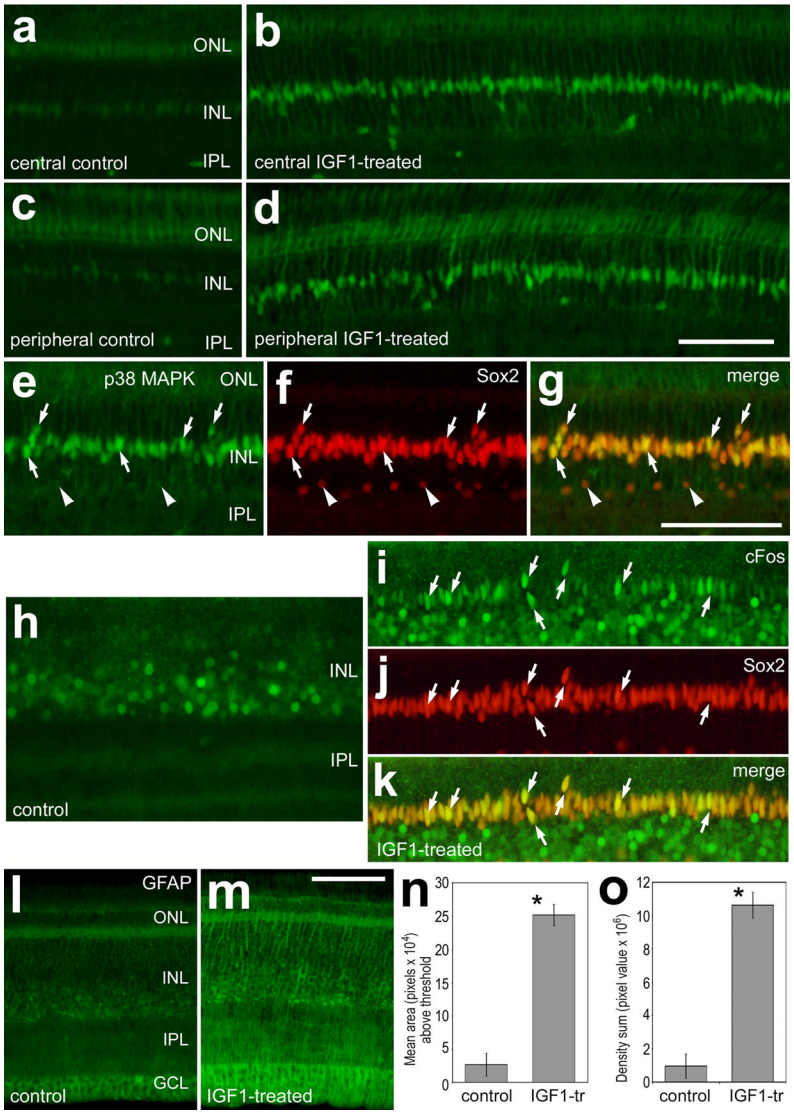

Figure 4.

IGF1 stimulates Müller glia to accumulate p38 MAPK, cFos and GFAP. Retinas were obtained from eyes that were treated with 2 consecutive daily injections of vehicle (**a**,**c**,**h** and **l**) or 2 consecutive daily injections of IGF1 (**b**,**d**,**e–g**,**i–k** and **m**) Vertical sections of the retina were labeled with antibodies to p38 MAPK (green in **a–e** and **g**), Sox2 (red in **f**, **g**, **j** and **k**), cFos (green in **h**, **i** and **k**), and GFAP (**l** and **m**). Images of the retina were obtained from central (**a**, **b**, and **e–m**) and peripheral (**c** and **d**) regions of the retina. Arrows indicate nuclei of Müller glia that are immunolabeled for p38 MAPK and Sox2 (**e–g**) or cFos and Sox2 (**i–k**). Arrow-heads indicate $Sox2^{+}$ amacrine cells that are negative for p38 MAPK. ImagePro 6.2 was used to measure total areas for pixel intensities >100 for GFAP (0 = black, 255 = saturated) and the density sum (total of pixel values within thresholded objects). Histograms (**n** and **o**) illustrate means (n=6) and standard deviations for the area and density sum for GFAP-immunofluorescence in control and IGF1-treated retinas. Significance of difference (*p<0.0001) was determined by using a two-tailed, unpaired Student's t-test. The calibration bar (50 μm) in panel **d** applies to **a–d**, the bar in **g** applies to **e–g** and **h–k**, and the bar in **m** applies to **l** and **m**.

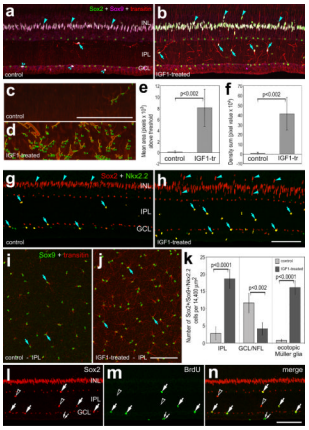

Figure 5.

IGF1 stimulates NIRG cells to up-regulate transitin, accumulate in the IPL, and proliferate. Retinas were obtained from eyes that received 2 consecutive daily injections of vehicle (**a**,**c**,**g** and **i**) or 800ng IGF1 (**b**,**d**,**h**,**j** and **l–n**). Vertical sections (**ad**, **g**, **h** and **l–n**) or whole-mounts (**i** and **j**) of the retina were labeled with antibodies to transitin (red in **a–d, i** and **j**), Sox9 (magenta in **a** and **b**; green in **i** and **j**), Sox2 (green in **a** and **b**; red in **g**, **h**, **l** and **n**), Nkx2.2 (green in **g** and **h**) or BrdU (**m** and **n**). ImagePro 6.2 was used to obtain measurements of total area for pixel intensities >100 for transitin (0 = black, 255 = saturated), and the density sum (total of pixel values within thresholded objects). In panels **c** and **d** the yellow outlines and green numbers indicate the areas designed by ImagePro 6.2 for each object that met the threshold criteria. Histograms in panels **e** and **f** illustrate IGF1-induced increases in transitin-immunofluoresence (area and density sum) in the IPL. The histogram in panel **k** illustrates the mean number of $Sox2^{+}/Sox9^{+}/Nkx2.2^{+}$ cells in the IPL or GCL/NFL, and Müller glia nuclei that are displaced distally away from the center of the INL in control and IGF1-treated retinas. Significance of difference (p-values) was determined by using a two-tailed, unpaired Student's t-test. Arrows indicate NIRG cells labeled for transitin, Sox9 or Sox2 in the IPL (**a**,**b**, **g–j**, and **l–n**) and arrow-heads indicate nuclei of Müller glia in the INL. In panels **l–n** arrows indicate $BrdU^{+}$ NIRG cells, small double-arrows indicate $BrdU^{+}/Sox2^{-}$ microglia, and hollow arrow-heads indicate $BrdU^{-}/Sox2^{+}$ NIRG cells in the IPL. The scale bar (50 μm) in panel **c** applies to panels **c** and **d**, the bar in **h** applies to **a**,**b**,**g** and **h**, the bar in **j** applies to I and j**,** and the bar in **n** applies to **l–n**.

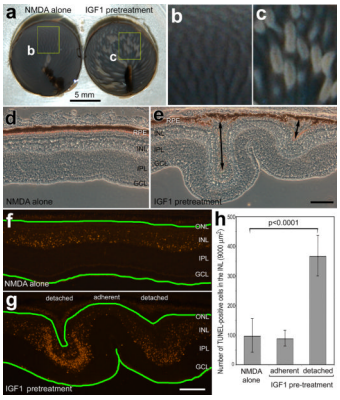

Figure 6.

IGF1-treatment exacerbates excitotoxic retinal damage. Retinas were obtained from eyes that received injections of vehicle (**b**,**d** and **f**) or IGF1 (**c**,**e** and **g**) at P5 and P6, NMDA at P7, and harvested at P8. Images of posterior eye-cups in panels **a–c** were obtained by using a digital SLR camera. The yellow boxes in panel **a** indicate regions that are enlarged 3-fold in panels **b** and **c**. The double-ended arrows in **e** indicate retinal detachments. The scale bar in panel **a** indicates 5 mm, the scale bar (50 μm) in panel **e** applies to panels **e** and **d**, and the bar (50 μm) in **g** applies to **f** and **g**. Vertical sections of the retina were imaged using phase contrast (**d** and **e**) or wide-field epifluorescence microscopy (**f** and **g**). The TUNEL method was used to label fragmented DNA *in situ* to identify dying cells. The histogram in panel **h** illustrates the means (n=6) and standard deviations. There was a significant difference in the number of $TUNEL^{+}$ cells in the INL of retinas treated with NMDA alone and in the INL of detached regions of retina treated with IGF1 before NMDA. Significance of difference (**h**) was determined by using a two-tailed, unpaired Student's t-test.

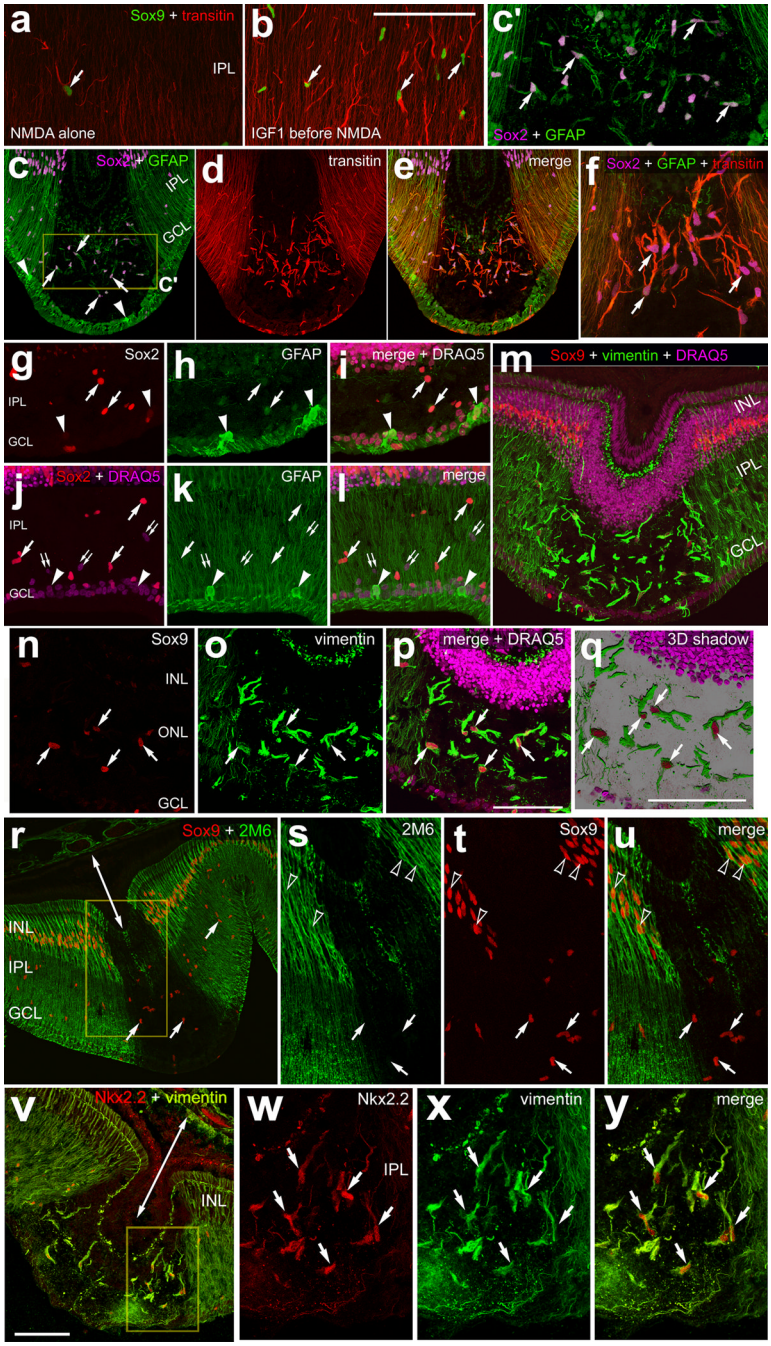

Figure 7.

IGF1-treatment before an excitotoxic insult results in retinal detachments that are associated with losses of Müller glia and accumulations of NIRG cells. Retinas were obtained from eyes that received injections of vehicle (**a**) or IGF1 (**b–y**) at P5 and P6, NMDA at P7, and harvested at P8. Vertical sections of the retina were labeled with antibodies to transitin (red in **a**, **b** and **d–f**), Sox9 (green in **a** and **b**; red in **m**,**n**,**p–r**,**t** and **u**), GFAP (green in **c**,**e**,**f**,**h**,**i**,**k** and **l**), Sox2 (magenta in **c**,**e** and **f**; red in **g**,**i**, **j** and **l**), vimentin (green in **m** and **o–q**), 2M6 (green; **r, s** and **u**) and Nkx2.2 (red nuclei in **v–y**). Nuclei were stained with DRAQ5 (magenta; **i**,**j**,**l**,**m**,**p** and **q**). The images in panels **a** and **b** were obtained using identical microscope settings. Panel **c**′ is a 2.5-fold enlargement of the area indicated by the yellow

box in panel **c,** panels **s–u** are 2-fold enlargements of the boxed-out area in **r**, and panels **w–y** are 2.5-fold enlargements of the boxed-out area in **v**. In panels **v–y**, sequential immunolabeling was used because the antibodies to Nkx2.2 and vimentin were both mouse monoclonals. The anti-Nkx2.2 and anti-IgG-Alexa568 were applied after the anti-vimentin and anti-IgG-Alexa488. Thus, the anti-IgG-Alexa568 labeled both primary antibodies, whereas the anti-IgG-Alexa488 labeled the anti-vimentin alone. Double-ended arrows indicate detachments of the photoreceptor layer from the RPE (**r** and **v**). Arrows indicate NIRG cells, arrowheads indicate $GFAP^+$ astrocytes (**g–l**), hollow arrow-heads indicate the nuclei of Müller glial (**s–u**) and small double-arrows indicate $DRAQ5^+$, Sox2-negative cells in the IPL (presumptive microglia; **j–l**). The calibration bar (50 μm) in panel **p** applies to panels **c′, g–l** and **n–p**, the bar in **q** applies to **a**,**b**,**f** and **q**, and the bar in **v** applies to **c–e**, **m**, **r** and **v**.

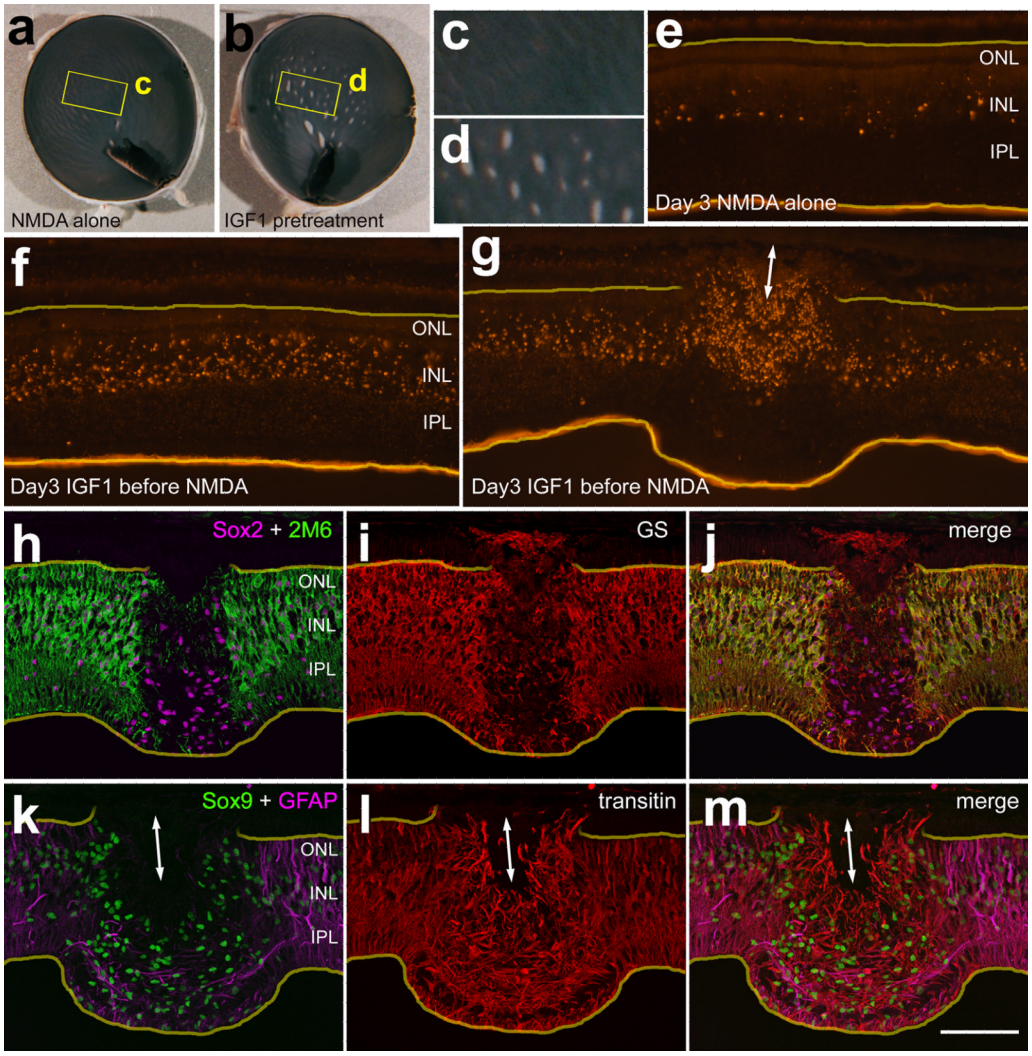

Figure 8.

Detached regions of retina lacking Müller glia are observed 3 days after NMDA with IGF1 pre-treatment. Retinas were obtained from eyes treated with NMDA alone (**a**,**c**,**e** and **n**) or NMDA with IGF1-pretreatment (**b**,**d**,**f–m**,**o** and **p**). Images were obtained using a digital SLR camera (**a–d**), wide-field epifluorescence microscopy (**e–g** and **n–p**), and confocal microscopy (**h–m**). Vertical sections of the retina were labeled for fragmented DNA using the TUNEL method (**e–g**), or antibodies to Sox2 (magenta in **h** and **j**), 2M6 (green in **h** and **j**), glutamine synthetase (red in **i** and **j**), Sox9 (green in **k** and **m**), GFAP (magenta; **k**), transitin (red; **l**), or biotinylated RCA1 (**n–p**). Yellow lines indicate the inner and outer limiting membranes (**e–m**). Double-ended arrows indicate detachments of the photoreceptor layer from the RPE (**g** and **k–m**). The calibration bar (50 μm) in panel **p** applies to panels **e–p**.

Table 1

List of antibodies, working dilution and sources.

Antigen	Host	Working Dilution	Clone or Catalog number	Source
Egr1	goat	1:1000	AF2818	R&D Systems
pERK1/2	rabbit	1:200	137F5	Cell Signalling Technologies
pCREB	rabbit	1:1000	87G3	Cell Signalling Technologies
p38 MAPK	rabbit	1:400	12F8	Cell Signalling Technologies
cFos	rabbit	1:400	K-25	Santa Cruz Immunochemical
Sox2	goat	1:1000	Y-17	Santa Cruz Immunochemical
Sox9	rabbit	1:2000	AB5535	Chemicon
Nkx2.2	mouse	1:50	74.5A5	Developmental Studies Hybridoma Bank
Islet1	mouse	1:50	40.2D6	Developmental Studies Hybridoma Bank
Brn3a	mouse	1:200	mab1585	Chemicon
BrdU	rat	1:200	OBT00030S	Serrotec
BrdU	mouse	1:80	G3B4	Developmental Studies Hybridoma Bank
glial fibrilliary acidic protein	rabbit	1:2000	Z0334	Dako
proliferating cell nuclear anitgen	mouse	1:1000	M0879	Dako
CD45	mouse	1:200	HIS-C7	CediDiagnostic
2M6	mouse	1:100	2M6	Dr. Paul Linser, U of Florida
glutamine synthetase	rabbit	1:1000	GS	Dr. Paul Linser, U of Florida
lysosomal membrane glycoprotein	mouse	1:50	LEP-100	Developmental Studies Hybridoma Bank
Pax6	mouse	1:500	PAX6	Developmental Studies Hybridoma Bank
transferrin binding protein	rabbit	1:5000	TFBP	Dr. J.J. Lucas, SUNY
transitin	mouse	1:50	EAP3	Developmental Studies Hybridoma Bank
transitin	mouse	1:600	7A3B5	Dr. Paul Henion, Ohio State University

Table 2

Summary of markers found in the different types of retinal glia

	oligodendrocytes	astrocytes	microglia	Muller glia	NIRG cells
Sox2	+	∅	∅	+++	+++
Sox9	+++	∅	∅	+++	+++
Nkx2.2	++	∅	∅	∅	+++
transitin	∅	∅	∅	+	+++
vimentin	∅	∅	∅	+++	+++
GFAP	∅	+++	∅	+	+
2M6	∅	∅	∅	+++	∅
TFBP	+++	∅	∅	∅	∅
GS	∅	∅	∅	+++	∅
RCA1	∅	∅	+++	∅	∅
CD45	∅	∅	+++	∅	∅
LMG	∅	∅	++	∅	∅

Abbreviations: GFAP – glial fibrilliary acidic protein, TFBP – transferrin binding protein, GS – glutamine synthetase, LMG – lysosomal membrane glycoprotein, + some/sparse labeling, ++ moderate labeling, +++ strong/abundant labeling, ∅ no labeling.

Glia. Author manuscript; available in PMC 2011 April 15.